The Engineering Society
For Advancing Mobility
Land Sea Air and Space
400 COMMONWEALTH DRIVE WARRENDALE, PA 15096

SAE Technical
Paper Series

871740

# Efficient Implementation of Random Pressure Fields with the Finite Element Method

**Philip J. Hipol and Allan G. Piersol**
Astron Research and Engineering
Santa Monica, CA

Aerospace Technology Conference
and Exposition
Long Beach, California
October 5-8, 1987

**ISSN 0148-7191**

# Efficient Implementation of Random Pressure Fields with the Finite Element Method

**Philip J. Hipol and Allan G. Piersol**
Astron Research and Engineering
Santa Monica, CA

## ABSTRACT

An efficient technique is developed for use with the finite element method for the vibration prediction of structures subjected to random, spatially distributed excitation pressure fields. User input to the finite element code and computation time are minimized by taking advantage of reciprocity within the finite element model. The technique is applied to a simple panel subjected to turbulent boundary layer and reverberent field excitations, and results are compared to those obtained through classical normal mode theory.

WITH THE INCREASING AVAILABILITY of large capacity, high speed digital computers, the application of finite element techniques to the prediction of aeroacoustic induced random vibration environments of aerospace vehicles is also increasing. An important requirement in such applications is the need to input an appropriate random, spatially distributed excitation pressure field to the finite element model in a computationally efficient manner. Three broad classes of excitation pressure fields are of common interest. The first is a propagating, sonic pressure field that is representative of jet noise generated during the take-off of an airplane, or the rocket noise produced during the lift-off of a launch vehicle. The second is a convecting pressure field that is representative of the turbulent boundary layer created on the exterior structure of the vehicle during operation at high flight dynamic pressures. The third is a diffuse pressure field which is representative of the reverberent acoustic field inside a payload bay or shroud.

## ANALYTICAL BACKGROUND

A review of the analytical formulation of vibration prediction considering the three classes of excitation random pressure fields is given. This review outlines the classical normal mode theory and its extension to the finite element method. A complete treatment of the analytical formulation is beyond the scope of the present effort, and the reader is advised to consult the references for details and derivations.

In the context of classical normal mode theory, the analytical formulation of the vibration prediction problem is straight-forward. For example, consider an arbitrary structure subjected to an arbitrary load, as illustrated in one dimension in Figure 1 (the solution readily extends to two dimensions). The auto (power) spectral density function for the vibration response at any point x on the structure is given by [1]*:

$$G_{zz}(x,f) = L^2 G_r(f) \left\{ \sum \sum \left[ \phi_i(x) \phi_j(x) H_i^*(f) H_j(f) j_{ik}^2(f) \right] \right\} \qquad (1)$$

where:

$$j_{ik}^2(f) = \left[ L^2 G_r(f) \right]^{-1} \left\{ \iint_0^L \phi_i(\alpha) \phi_k(\beta) G_{p\alpha p\beta}(\alpha,\beta,f) \, d\alpha \, d\beta \right\} \qquad (2)$$

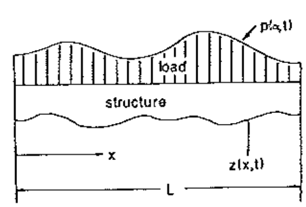


Figure 1. Continuous Structure with Distributed Excitation

* Numbers in brackets denote references at end of paper

0148-7191/87/1005-1740$02.50

The expression given by Equation (2) is called the "cross-acceptance function" (essentially "Green's function"), and involves an integration of the product of modal deflections and cross-spectral density functions of the presure field over all points on the structure, $\alpha$ and $\beta$, where the load is applied.

The key to vibration prediction is the definition of the normal modes of the structure and the cross-spectral density function for the applied load. Assuming the load is a homogeneous pressure field, the cross-spectrum can be defined as a function of separation distance, $\Delta x$, rather than the specific points, $\alpha$ and $\beta$, that is,

$$G_{p\alpha p\beta}(\alpha,\beta,f) = G_{12}(\Delta x,f) \quad (3)$$

Experience suggests [2] that the cross-spectrum for pressure fields due to jet noise and aerodynamic boundary layers can be approximated in two dimensions by:

$$G_{12}(\Delta x,\Delta y,f) = \exp(-a_x|\Delta x|)\cos(k_x\Delta x) * \exp(-a_y|\Delta y|)\cos(k_y\Delta y) \quad (4)$$

where a is an exponential weight, and k is the wave number given by the radian frequency divided by the trace velocity. For the case of pressure fields generated by jet and rocket noise, the trace velocity is given by:

$$v_x = c / \sin\theta_x \qquad v_y = c / \sin\theta_y \quad (5)$$

where c is the speed of sound, and $\theta$ is the angle of incidence relative to the normal to the structure. For the case of pressure fields generated by the turbulent boundary layer on a vehicle moving along the x axis, the trace velocity v is a convection velocity that is commonly approximated by [4]:

$$v_x = 0.8\,U_\infty \qquad v_y = \infty \quad (6)$$

where $U_\infty$ is the free stream velocity of the vehicle.

For reverberant acoustic fields, the cross-spectrum of the pressure field is often approximated by a diffuse noise model [3] of the form:

$$G_{12}(\Delta x) = \sin(k\Delta x)/(k\Delta x) \quad (7)$$

where k is the radian frequency divided by the speed of sound. For this model, the cross-spectra along the x and y axes are identical.

Now consider the case where an excitation pressure field must be applied at discrete points on the structure, as is appropriate for finite element applications. Assuming that there are q discrete input points, as illustrated in Figure 2, Equation (1)

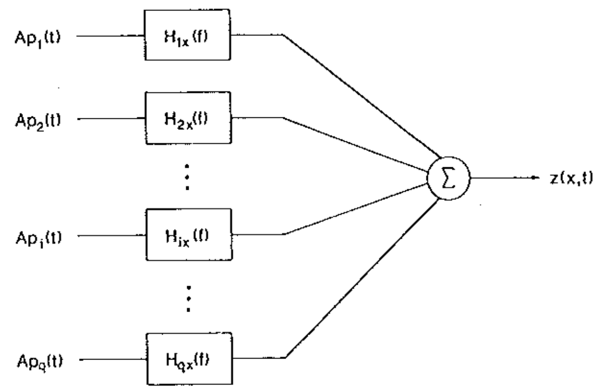


Figure 2. Finite Element Model with Discrete Excitation

can be replaced by [5]:

$$G_{zz}(x,f) = \sum_{i=1}^{q}\sum_{j=1}^{q} H_{ix}^{*}(f)G_{ij}(f)H_{jx}(f) \quad (8)$$

Equation (8) then becomes the basic working relationship to calculate the response of a structure to a distributed load defined by a matrix of cross-spectra, which represent the discrete version of the load defined in Equations (4) and (7).

## FINITE ELEMENT IMPLEMENTATION

Finite element methods have been applied to obtain the response of linear elastic structures to random pressure fields through numerous past efforts [6]. Since a comprehensive review of the literature is beyond the scope of the present effort, a brief summary is provided which outlines the key aspects of these methods. Following this summary is a discussion of modifications which can be made to the basic random response solution algorithm to greatly enhance its computational efficiency in the solution of this class of problem.

The auto-spectral density function is typically normalized to a unit pressure auto spectral density acting over the entire structure. Finite element codes [7,8] require the discretization of pressure fields into work equivalent forces which act on each of the model grid points. For a model with arbitrary grid point spacing, element size, or element type, these grid point forces vary in magnitude, although the pressure over the entire model is uniform when the local area at each grid point, or the element assumed displacement field, is considered.

The grid point forces are applied to the finite element model in a successive manner, and at each discrete frequency of interest, grid point complex displacements are computed through frequency response analysis in a modal or direct formulation [8]. The collection of complex displacements due to the application of a grid point force at a given location defines a complex displacement vector which becomes a column in the frequency response function matrix. After all of the grid point forces have been evaluated, the frequency response function matrix is assembled through the collection of complex displacement vectors. Note that a model with q grid points requires the calculation of q work equivalent forces and q passes through frequency response analysis to completely define the frequency response function matrix at each discrete frequency of interest.

Correlation between each pair of grid point forces is obtained through the calculation of cross-spectral density matrices. For the three classes of excitation pressure fields described above, the cross-spectra are a function of excitation frequency and grid point separation distance. Separation distances are calculated between each grid point in the model in each direction of interest. These separation distances are then used in Equation (4) or (7) to compute the cross-correlation coefficients. Since the cross-spectral density matrix must be hermitian, only the upper triangle of the matrix is generated.

The auto-spectral density is calculated through the application of Equation (8). At each discrete frequency, the appropriate cross-spectral density matrix between two discrete points is pre- and post- multiplied by the corresponding frequency response functions between the input points and the response location. The summation of matrix products over the entire finite element model yields the auto spectral density at a discrete frequency.

The standard finite element formulation for random analysis as described above is not ideally suited for problems involving random pressure fields. It can be seen that this formulation is cumbersome due to the fact that work equivalent forces must be defined for each finite element grid point, and separate passes through frequency response analysis must be conducted for each force to generate the frequency response function matrix at each discrete frequency. For larger models involving complex geometry and arbitrary grid spacing, element size, or element type, user input in defining each grid point force and the cross correlation coefficients between each force can be untenable. Furthermore, the standard formulation is computationally intensive due to the large amount of I/O and matrix operations required for each successive frequency response analysis.

It is possible to greatly simplify the finite element method in the solution of this class of problem by recognizing that reciprocity must exist for linear elastic structures. The frequency response function matrix can be generated through analysis with only one grid point force applied to the response location on the finite element model (although this location is actually arbitrary). The resulting complex displacement vector can be used to create the entire frequency response function matrix since it is a scalar multiple of all other complex displacement vectors obtained through analysis of forces applied to other points on the model. Since it is necessary to maintain a unit pressure loading over the entire model, this scalar multiple is defined by the ratio of the nodal area at the response location to the nodal area at the respective input location. Since the frequency response function matrix must be hermitian, only the upper triangle of the matrix must be calculated. Equation (8) is therefore modified as follows:

$$G_{zz}(x,f) = \sum_{i=1}^{q}\sum_{j=1}^{q} H_{ix}^{*}(f)\,\frac{A_x}{A_i}\,G_{ij}(f)H_{jx}(f)\,\frac{A_x}{A_j} \quad (9)$$

Application of Equation (9) enhances the computational efficiency of the random response solution algorithm by requiring the input of only one grid point force to the finite element model at the response location, requiring only one frequency response analysis, and the determination of only one complex displacement vector for each discrete frequency of interest. Both user input and computation are greatly reduced as a result.

The schematic diagram which describes the implementation of random analysis using Equation (9) is shown in Figure 3. This method differs from the standard formulation described above since random analysis is performed with an external Fortran code. A frequency response analysis is performed with one grid point force, and the resulting complex displacement vectors are written to file. The external random analysis program reads the finite element geometry to calculate grid point separation distances and nodal areas. The separation distances are used in either Equation (4) or (7) to generate the cross-spectral density matrices, and nodal areas are used in conjunction with the complex displacement vectors to generate the frequency response function matrices. The auto spectral density is then calculated over the entire frequency range with Equation (9). These results are then provided in tabular and plottable formats.

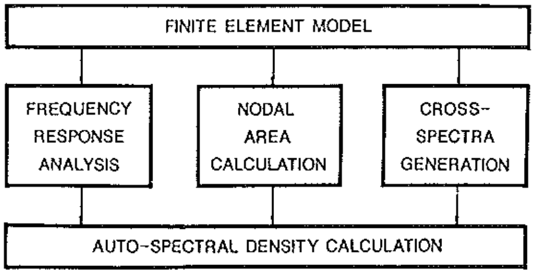


Figure 3. Random Analysis Solution Schematic Layout

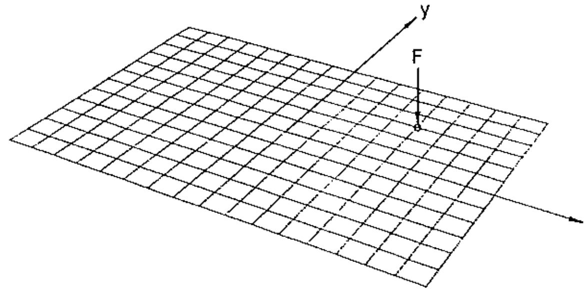


Figure 4. Force Applied to Quarter Point of Plate Model

## EXAMPLE APPLICATIONS

The finite element method described above was implemented to obtain the response of a clamped plate subjected to a turbulent boundary layer excitation, and a simply supported plate subjected to a reverberent field excitation. Finite element results were then compared to the classical normal mode solutions for these problems.

The finite element model of the plate can be seen in Figure 4. This model contains 221 grid points and 192 linear displacement elements. Each element was given the physical and material properties defined in Table 1.

Table 1. Plate Properties

| | |
|---|---|
| $L_1$ | 0.0064 m (0.25 in) |
| $L_2$ | 0.0058 m (0.23 in) |
| $t$ | 0.000381 m (0.015 in.) |
| $E$ | 232.3 GPa (33.7 msi) |
| $\nu$ | 0.30 |
| $\eta$ | 0.009 |
| $\rho$ | 7473.0 kg/m$^3$ (0.27 lb/in$^3$) |

The flow parameters for the turbulent boundary layer excitation were defined with a free-stream Mach number of 0.3, and a displacement boundary-layer thickness of 0.00454 m (0.179 in.) Equations of the form given by (4) were implemented to obtain the cross-spectrum of the pressure field, where the convection velocity was given by equations of the form given by (6). Details are provided in [4]. All edges of the plate were initially constrained in all degress of freedom (clamped boundaries), and the response location was defined at the plate quarter point (Figure 4). A work equivalent unit pressure force was applied to the response location, and a modal frequency response analysis [8] was conducted up to 2000 Hz. This analysis involved 74 discrete frequencies and five normal modes.

For the reverberent field excitation, Equation (7) was directly implemented to obtain the cross-spectrum of the pressure field. The initial plate boundary conditions were modified by allowing for in-plane rotation (simply-supported boundaries). A work equivalent unit pressure force was applied to the response location, and a modal frequency response analysis [8] was conducted up to 2000 Hz. This analysis involved 117 discrete frequencies and eight normal modes.

Finite element results for the turbulent boundary layer and reverberent field excitation are shown in Figures 5 and 6. These results are plotted against the classical normal mode solutions given by [4] and [9], respectively. It should be noted that the classical normal mode solutions assume only plate bending stiffness, whereas the finite element solutions include plate bending, membrane, shear and coupling stiffnesses. These results show that there is very good agreement between the methods for lower mode orders; however there is some degradation of the finite element solution at the higher mode orders. This degradation is attributed to insufficient refinement of the finite element mesh, and will be less prevalent with a higher degree of mesh refinement.

## CONCLUSIONS

The standard finite element solution [8] for random analysis involving distributed pressure fields can be simplified by considering reciprocity of the complex displacement vector between points on the model at discrete frequencies of interest. Both user input to the finite element code and computation time are minimized since the simplified method requires the definition of only one load and one pass through frequency response analysis. This method was shown to be effective in predicting the response of a simple plate to both turbulent boundary layer and reverberent excitation fields.

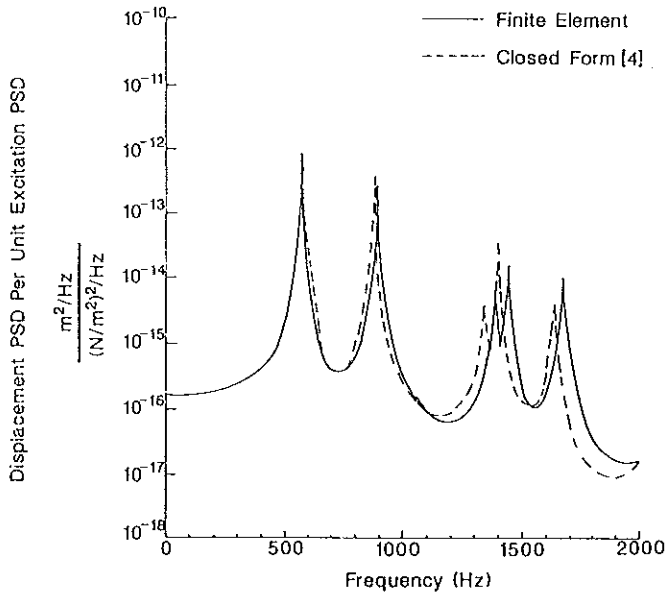


Figure 5. Response Due to Turbulent Boundary Layer Excitation

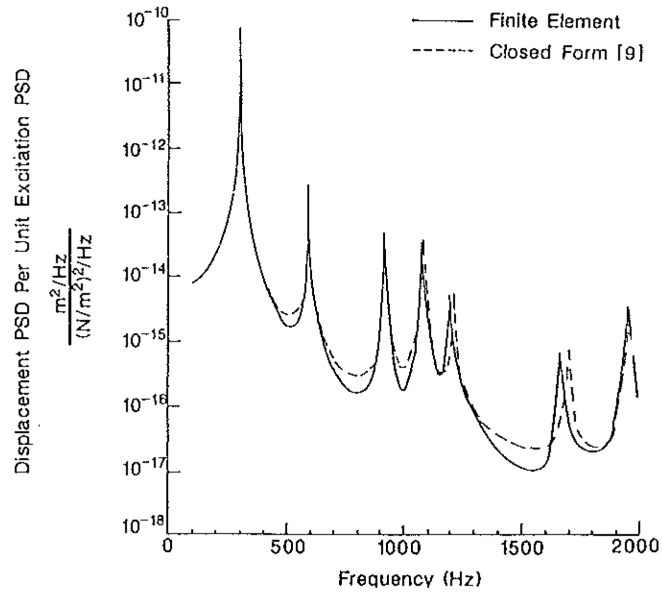


Figure 6. Response Due to Reverberent Field Excitation

NOMENCLATURE

| | |
|---|---|
| $A_i$ | nodal area at ith grid point |
| $A_x$ | nodal area at response location |
| c | speed of sound |
| E | Young's modulus |
| f | frequency |
| $G_{ij}(f)$ | cross-spectral density function between ith and jth discrete inputs |
| $G_{p\alpha p\beta}(\alpha,\beta,f)$ $G_{i_2}(\Delta x,f)$ | cross-spectral density function |
| $G_r(f)$ | reference spectral density function |
| $G_{zz}(x,f)$ | auto-spectral density function |
| $H_i(f)$ | generalized frequency response function for the ith normal mode |
| $H_{ix}(f)$ | frequency response function between ith discrete input and response location |
| $j^2_{ik}(f)$ | cross-acceptance function |
| k | wave number (2 f/v) |
| L | length |
| $L_1$ , $L_2$ | lengths in x and y directions |
| x | response point |
| $\Delta x$ , $\Delta y$ | separation distances |
| t | thickness |
| U | free stream velocity |
| v | trace or convection velocity |
| * | complex conjugate |
| $\alpha$, $\beta$ | spatial coordinates |
| $\phi_i$ | mode shape for the ith normal mode |
| $\nu$ | Poisson's ratio |
| $\eta$ | loss factor |
| $\rho$ | density |
| $\theta$ | angle of incidence |

ACKNOWLEDGEMENT

The authors wish to acknowledge the contributions of J.F. Wilby and E.G. Wilby of Astron Research and Engineering, Santa Monica, California, and S.A. McInerny of the Aerospace Corporation, El Segundo, California.

REFERENCES

1. Bendat, J. S., and Piersol, A. G., Engineering Applications of Correlation and Spectral Analysis, p. 119, Wiley, New York, 1980.
2. Cockburn, J. A., and Jolly, A. C., "Structural-Acoustic Response of an Aircraft Fuselage Excited by Random Pressure Fields", AFFDL-TR-68-2, Wright-Patterson AFB, OH, 1968.
3. Morrow, C.T., "Point-to-Point Correlation of Sound Pressures in Reverberent Chambers", Shock and Vibration Bulletin, No. 39, 1969.
4. Chyu, W.J., and Au-Yang, M.K., "Random Response of Rectangular Panels to the Pressure Field Beneath a Turbulent Boundary Layer in Subsonic Flows", NASA TN D6970, Ames Research Center, Moffet Field, CA, Oct. 1972.
5. Bendat, J. S., and Piersol, A. G., Random Data: Analysis and Measurement Procedures, p. 245, Wiley, New York, 1968.
6. Jacobs, L.D., Lagerquist, D.R., and Gloyna, F.L., "Response of Complex Structures to Turbulent Boundary Layers", AIAA Paper No. 69-20, AIAA New York, 1969.
7. Zienkiewicz, O. C., The Finite Element Method, p. 234, McGraw-Hill, London, 1977.
8. MacNeal, R.H. (Editor), The NASTRAN Theoretical Manual, MacNeal-Schwendler Corporation, Los Angeles, 1972.
9. Wilby, J.F, and Wilby E.G., unpublished data, Astron Research and Engineering, Santa Monica, CA, 1987.

Printed in U.S.A.